Native Mass Spectrometry Analysis of a Cullin RING Ubiquitin E3 Ligase Complex in the Context of Targeted Protein Degradation

Louise M Sternicki[1, 2,*], Charlotte Crowe[3], Alessio Ciulli[3], Sally-Ann Poulsen[1, 2,*]

*Email: l.sternicki@griffith.edu.au; s.poulsen@griffith.edu.au

Affiliations

[1]Institute for Biomedicine and Glycomics, Griffith University, Gold Coast, Queensland 4222, Australia

[2]School of Environment and Science, Griffith University, Brisbane South (Nathan), Queensland 4111, Australia

[3]Centre for Targeted Protein Degradation, School of Life Sciences, University of Dundee, Dundee DD1 5JJ, United Kingdom

Abstract

The binding of PROTACs to their partner ubiquitin E3 ligase (E3) and a protein of interest (POI) is critical for PROTAC development and validation. Characterisation of PROTAC complexes by cryo-electron microscopy and X-ray crystallography is not always feasible, especially where species may be transient and protein structures may not resolve due to flexible domains or intrinsically disordered regions. More routine biophysical methods with broader applicability to varied samples is desirable to support the rapidly expanding targeted protein degradation field. The majority of PROTACs in development and in the clinic act through a Cullin RING E3 ligase (CRL) of which the pentameric von Hippel-Lindau (VHL) Cullin 2 RING E3 complex $CRL2^{VHL}$ is the foundational example. Native mass spectrometry (nMS) can be used to characterise protein complexes but has not previously been used to characterise a full E3 or any E3-E2 interactions. Here, we show that $CRL2^{VHL}$ is amenable to characterisation by nMS and its interactions can be observed by the mix-and-matching with the other protein components integral to the targeted protein degradation mechanism. Specifically, we characterise binary, ternary and higher order complexes that comprise $CRL2^{VHL}$ and the PROTAC MZ1, including the multiprotein systems of POI-PROTAC-$CRL2^{VHL}$, $CRL2^{VHL}$-E2-Ub, and POI-PROTAC-$CRL2^{VHL}$-E2-Ub, all of which are essential in the lead up to productive POI ubiquitination and degradation. We anticipate that our findings will be readily transferable to other full E3s and that nMS may open alternative avenues to characterising complex high mass multiprotein interactions.

Introduction

The ubiquitin–proteasome system (UPS) is responsible for cellular protein degradation. It acts by covalently attaching ubiquitin (Ub), a 76 amino acid protein, to a lysine residue of the substrate protein via a three-enzyme cascade with a ubiquitin-activating enzyme (E1), a ubiquitin-conjugating enzyme (E2) and a ubiquitin ligase (E3). The E3 catalyses the transfer of Ub from the E2 to the target substrate, which then directs it to the proteasome for degradation, **Figure 1**.[1] It is possible to manipulate the UPS with small molecules called degraders that are designed to simultaneously bind an E3 and a protein of interest (POI), **Figure 1**.[2-4] When applied for biological or therapeutic interventions this approach, known as targeted protein degradation, provides an almost unlimited scope to degrade any cellular protein and degrader development is a rapidly expanding field.[2-5] There are two well established categories of degrader molecules - PROTACs and molecular glues. They are distinctly different in architecture as PROTACs comprise two linked parts; the first part is a pharmacophore that binds the POI and the second part is a pharmacophore that binds to an E3, while molecular glues are made up from a single part that recognises both the POI and E3. Formation of a POI-degrader-E3 ternary complex followed by coordination to an E2 loaded with Ub (E2-Ub) is essential for ubiquitination.[6] Despite the importance of the full POI-degrader-E3-E2-Ub complex for the proximity and orientation of the POI relative to the donor Ub, there are few structural studies that have captured this species. Furthermore, workflows to capture the multiprotein species of ubiquitination with native proteins at scale are lacking. This limits routine direct assessment of structural and mechanistic features of degrader-mediated protein complexes relevant to a degrader's pharmacological activity.[6]

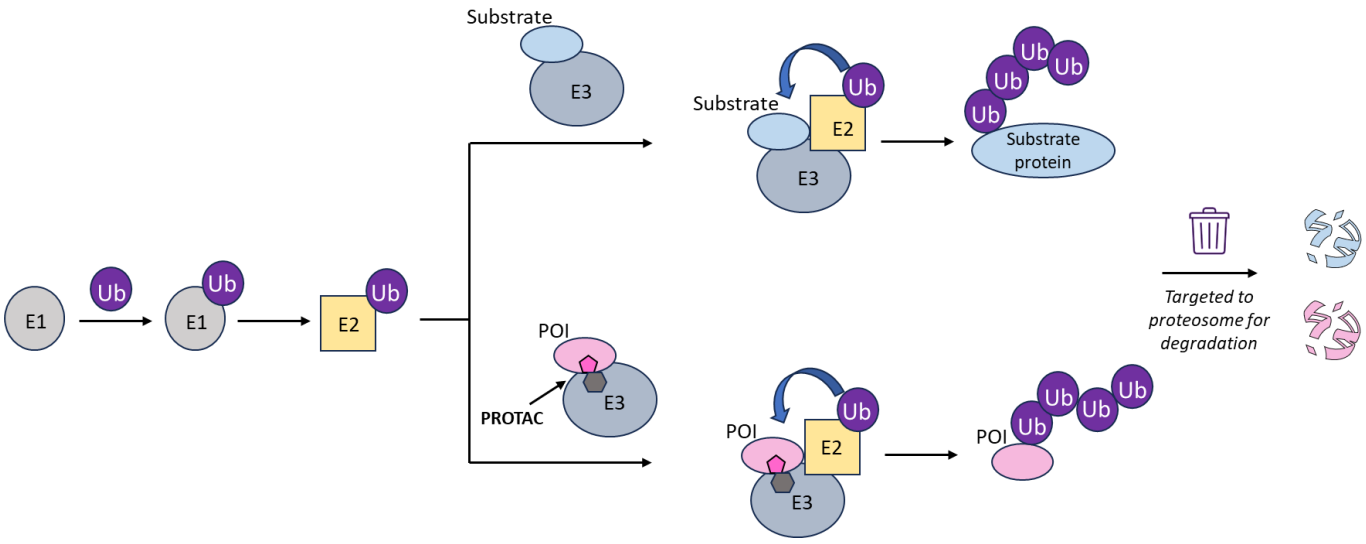

Figure 1. Schematic overview of (top path) the ubiquitin–proteasome system (UPS) three-enzyme cascade with a ubiquitin-activating enzyme (E1), a ubiquitin-conjugating enzyme (E2) and a ubiquitin ligase (E3), and (bottom path) mechanism of action of targeted protein degradation via hijacking the UPS with PROTAC molecules.

There are >600 human E3 ligases with the Cullin RING ligase (CRL) E3 subfamily the most abundant.[7, 8] CRLs are modular multiprotein complexes, comprising a Cullin scaffold protein (Cul1 – Cul5, Cul7 or Cul9), adaptor proteins (e.g. SKP1, EloB, EloC and/or DDB1), a RING-box protein (Rbx1 or Rbx2) that recruits the E2 enzyme loaded with Ub and a substrate-receptor protein that recruits the substrate protein that is for eventual degradation.[1, 7, 8] Most reported structural studies of POI-degrader-E3 ternary complexes utilise the minimal E3 ligase VCB, this is a trimeric species comprising VHL (Von Hippel-Lindau protein) as the substrate-receptor protein with EloB (elongin B) and EloC (elongin C) as adapter proteins, most notably it is without a Cullin scaffold protein or RING-box protein so cannot interact with E2-Ub.[9] Although robust (VCB is readily expressed and has excellent stability) there are drawbacks to this minimal approach as the measured ternary complex binding is relatively far removed from the downstream biological activity sought in degrader development. The focus of the present manuscript is native mass spectrometry (nMS) analysis of $CRL2^{VHL}$, the foundational full E3 ligase that has been central in development of functional degraders. $CRL2^{VHL}$ is a pentameric protein complex comprising VCB (a VHL-EloB-EloC trimer), Cul2 and Rbx1. The advantage of using this full E3 over VCB alone in interaction studies with PROTACs is that it is a functionally active version of the E3 that can recruit both the substrate protein (POI) and the E2-Ub. Specifically, we explore analysis of

CRL2^{VHL}, the corresponding ternary complex with MZ1 (as PROTAC) and BRD4^{BD2} (as POI),[10] the CRL2^{VHL}-E2-Ub interaction and the full POI-PROTAC-CRL2^{VHL}-E2-Ub complex. As it is increasingly important to comprehensively characterise such multimeric complexes to more systematically support degrader development[11] our goal was to capture the interactions of the full E3 with the PROTAC and all the protein partners responsible for ensuring successful Ub transfer to the POI. We show how this depth of analysis could be achieved rapidly with nMS in a single mass spectrum from a single sample, with simultaneous observation of all equilibrium species. This is not possible with other biophysical methods. We employed *cis*-MZ1 as a PROTAC negative control across the various sample combinations, this further demonstrated the 'everything is visible' benefits of nMS analysis for application to targeted protein degradation technologies. The ligand chemical structures for this study are shown in **Figure 2.**

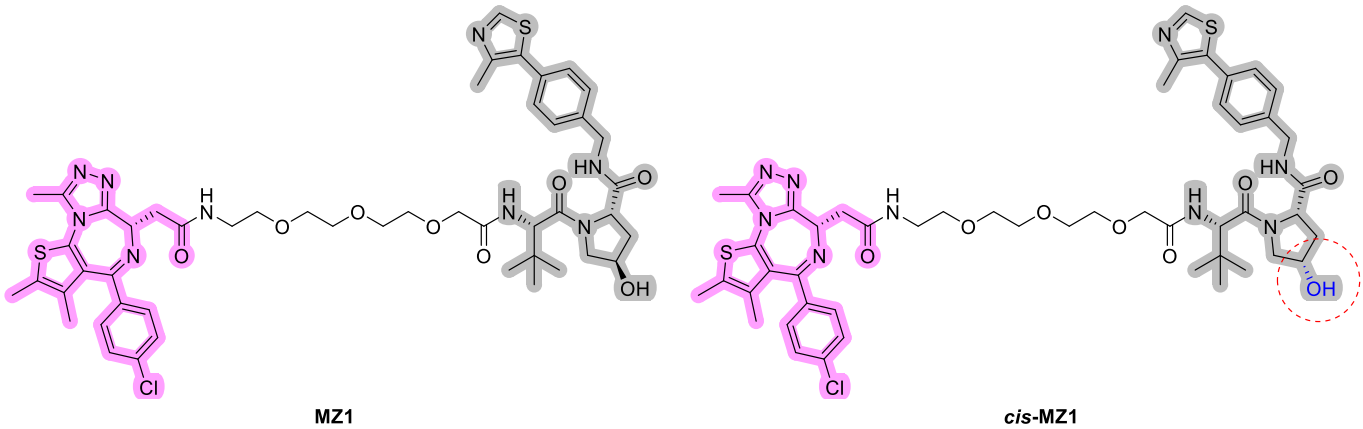

Figure 2. Structures of MZ1, a PROTAC that recruits VHL (grey, pharmacophore from VHL inhibitor VH032) and BRD4^{BD2} (pink, pharmacophore from BRD4^{BD2} inhibitor JQ1) and *cis*-MZ1, a negative control with no measurable binding affinity (as determined by ITC)[10] for VHL owing to the inverted stereochemistry of the hydroxyl group (red circle) compared to MZ1.[10]

Methods

Protein and ligand samples. BRD4^{BD2}, VCB, UBE2R1(C93K) and UBE2R1(C93K)-Ub samples were obtained from a previous study.[12] CRL2^{VHL} production is provided in **Supporting Information**. The test compounds MZ1 (PROTAC) and *cis*-MZ1 (negative control) were provided as dry stocks from opnMe, the

open science portal of Boehringer Ingelheim.[13] The compounds were solubilised to 10 mM in DMSO and the compound stock solution stored at -80 °C.

Native mass spectrometry sample preparation. Proteins were individually buffer exchanged into 150 mM ammonium acetate pH ~6.7 (Thermo Fisher AM9070G) using Micro Bio-Spin P-6 columns (Bio-Rad) according to manufacturer's protocols. Protein concentration following buffer exchange was determined by measuring the absorption at 280 nm and considered the protein's molecular weight and extinction coefficient (protein construct sequences provided in **Supporting Information**, **Table S1**). Compound stocks (10% DMSO) were prepared from the parent 100% DMSO stocks to yield a concentration that allowed a further 1/10 dilution into the nMS sample to give the desired compound test concentration for nMS at 1% DMSO (or less). Proteins were diluted in 150 mM ammonium acetate pH ~6.7 to the required concentrations and mixed with their protein binding partners as required, dependent on the test sample composition. Final concentrations of all test components are indicated for each sample/spectrum. All samples were incubated for at least 30 minutes at room temperature prior to nMS analysis.

Native mass spectrometry acquisition and data analysis. All nMS analysis was completed using a Q-Exactive Ultra High Mass Range Hybrid Quadrupole-Orbitrap Mass Spectrometer (UHMR MS, Thermo Fisher Scientific). Samples were introduced in the positive ion mode via either nanoelectrospray ionisation (nanoESI) from commercial borosilicate emitters with Au/Pd double coating (Thermo Fisher Scientific ES388, 1.1 mm tip length) or using a TriVersa NanoMate nanoESI source (Advion Biosciences) with a chip containing 5 µm diameter nozzles. nanoESI parameters for the borosilicate emitters included a spray voltage of 0.8-1.4 kV, and for the NanoMate source included a voltage of 1.7 kV and gas pressure of 1 psi. UHMR MS parameters were optimised to maximise signal intensity and signal-to-noise whilst maintaining intact folded proteins and protein complexes, and were in the range of values as follows: resolution 6,250 to 200,000, scan ranges 1,500-6,500, 1,500-8,000 or 2,000-10,000 *m/z*, microscans 5 or 10, averaging 5 or 20, capillary temperature 230 to 275 °C, S-lens RF level 200, desolvation voltage 0 to 60 V, trapping gas pressure 1.0 to 4.0, extended trapping 1.0, ion transfer target *m/z* set for high *m/z*, detector *m/z* optimisation set for low *m/z*,

nitrogen as the collision gas, data acquired for at least 1-2 minutes. Specific parameters for methods used for measuring different proteins and/or protein complexes are detailed in **Supporting Information**, **Table S2**. nMS data were analysed directly using Themo Fisher Scientific FreeStyle 1.8 SP2 QF1 and deconvoluted in UniDec.[14] UniDec data processing parameters were as follows: *m/z* range set to the full *m/z* range acquired, 3 to 7-40 charge state range, 10,000 to 50,000-200,000 Da MW range (charge state and MW range dependent on the sample), sample mass every 1 Da, peak detection range and threshold of 500 Da and 0.05 or 0.1, respectively. For accurate MW determination, the peak detection range was iteratively reduced to as low as 10 Da to identify the MW of the left-most unadducted peaks. To further identify low intensity species in deconvoluted mass spectra, the peak threshold was lowered to 0.02-0.03 as required. Specific UniDec deconvolution parameters for each protein and/or protein complexes measured are details in **Supporting Information**, **Table S2**.

Results and Discussion

Native mass spectrometry analysis of individual proteins and binary complexes. Native mass spectrometry (nMS) is well developed for characterising biomolecular interactions, including protein-small molecule and protein-protein interactions that underpin larger protein complexes.[15-18] nMS has been used in a small number of studies to characterise CRLs (without PROTAC)[19, 20] or PROTAC binary and ternary complexes with a minimal E3,[21-23] however no nMS studies are yet to characterise complexes with a full E3 comprising the Cullin scaffold and RING protein in the context of targeted protein degradation. Given the critical importance of the full E3 species in the mechanism of targeted protein degradation we were keen to address this gap. Recently, cryo-EM structures of the ternary complex of $CRL2^{VHL}$, MZ1 and $BRD4^{BD2}$ ($BRD4^{BD2}$-MZ1-(NEDD8)-$CRL2^{VHL}$) and the covalently crosslinked (for stability of an otherwise transient species) complex with the E2 UBE2R1 ($BRD4^{BD2}$-MZ1-(NEDD8)-$CRL2^{VHL}$-UBE2R1(C93K)-Ub) were reported (PDB 8RWZ and PDB 8RX0, respectively), **Figure 3**.[12] When compared to the minimal ternary complex with VCB (PDB 5T35, **Figure 3**) the cryo-EM structures revealed the conserved engagement of $BRD4^{BD2}$ with the VHL component of $CRL2^{VHL}$ in addition to a tilted and reoriented alignment of $BRD4^{BD2}$ distal to the MZ1-VHL binding interface toward the Rbx1, reducing the distance between the substrate protein

and the catalytic portion of the E3 for ubiquitination.[12] The observations made from analysis of the cryo-EM structures confirm the significance of using the whole native catalytic enzymatic machinery for investigating more detailed and nuanced mechanistic associated features for ubiquitination of the PROTAC-recruited target protein. *In vitro* ubiquitination assays and mass spectrometry profiling validated the predominant E2 UBE2R1 ubiquitinated lysine residues of BRD4^{BD2} was consistent with the cryo-EM structures.[12]

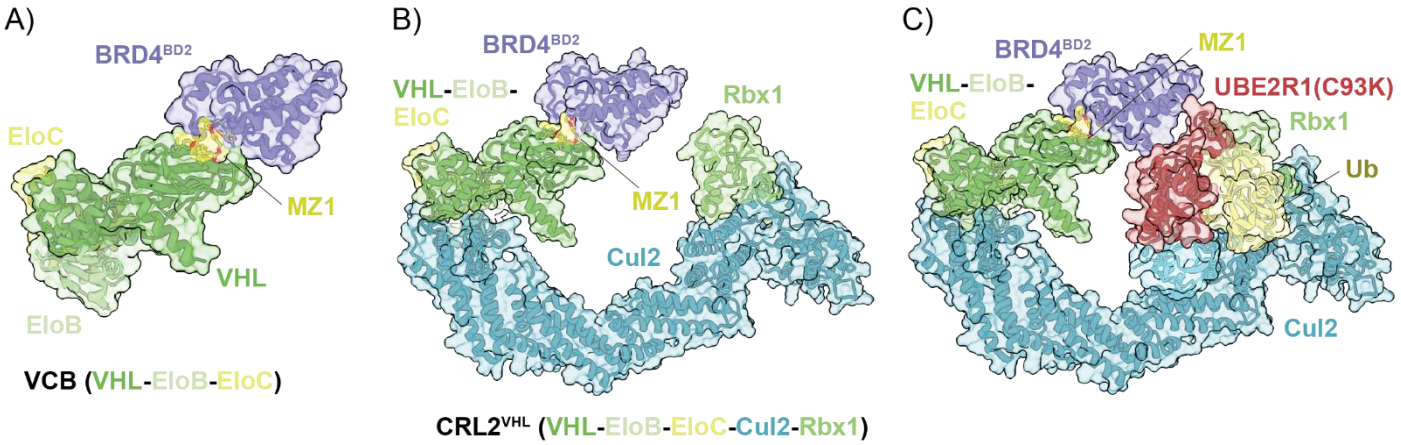

Figure 3. A. X-ray structure of minimal E3 ternary complex BRD4^{BD2}-MZ1-VCB (PDB 5T35). B. Cryo-EM structure of full E3 ternary complex BRD4^{BD2}-MZ1-CRL2^{VHL} (PDB 8RWZ). C. Cryo-EM structure of BRD4^{BD2}-MZ1-CRL2^{VHL}-E2-Ub covalently crosslinked complex (PDB 8RX0).[12, 24]

Prior to assessment of the sample compositions of interest, the individual protein components BRD4^{BD2}, VCB, CRL2^{VHL}, UBE2R1(C93K), and UBE2R1(C93K)-Ub, were first analysed by nMS to confirm sample identity, assess sample purity and to provide control spectra to support the analysis of the anticipated more complex mass spectra for mixed samples. All proteins were observed as a single dominant species with high purity, **Supporting Information**, **Figure S1, Table S3** and **Table S4**. The measured MW for BRD4^{BD2}, VCB and UBE2R1(C93K) agreed with the expected MW based on the protein construct sequences, **Supporting Information**, **Table S1**. The measured MW of the pentameric CRL2^{VHL} E3 ligase was ~175.5 Da higher than expected (observed 141,007 Da, expected based on protein construct sequence 140,831.5 Da), this may be attributed to three zinc cations as present in the cryo-EM structures PDB 8RWZ and PDB 8RX0, or other adducts of this larger multiprotein species. The observed MW of the E2-ubiquitinating conjugate protein with

Ub, UBE2R1(C93K)-Ub, was ~964 Da larger than expected (observed 36,247 Da, expected 35,283.5.4 Da) based on the protein sequence and likely corresponded to the addition of extra N-terminal residues of Ub, as previously characterised via denaturing LC-MS[12] (data not shown). The LC-MS measured mass was consistent with the MW determined by nMS. The UBE2R1(C93K)-Ub nMS spectrum contained a second minor species (observed 26,630 Da, ~9.6%) that corresponded to the protein without Ub covalently attached (expected MW 26,631 Da), **Supporting Information**, **Figure S1(E)**.

The noncovalent interactions of the protein components of VCB (minimal E3) and $CRL2^{VHL}$ (full E3) were assessed with in-source collision-induced dissociation (CID), by increasing the desolvation voltage. Under CID conditions of -75 V, VCB (trimeric VHL-EloC-EloB, 41,373 Da) dissociated into subunits of VHL-EloC (29,639 Da), EloC-EloB (22,696 Da) and VHL (18,675 Da). Free EloC (10,964 Da) and free EloB (11,733 Da) were the only potential dissociation species not observed, **Supporting Information**, **Figure S2** and **Table S5**. Increasing the CID conditions to -150 V resulted in the observation of all possible subunit dissociation products from VCB, these include VHL-EloB (30,408 Da), VHL-EloC (29,639 Da), EloC-EloB (22,695 Da), VHL (18,675 Da), EloB (11,732 Da) and EloC (10,962 Da). In-source CID (-75 V) of $CRL2^{VHL}$ (pentameric VHL-EloB-EloC-Cul2-Rbx1, 141,007 Da) resulted in the observation of Cul2-Rbx (observed 99,583 Da, ~125 Da higher MW than expected MW 99,458 Da), VCB (VHL-EloC-EloB, 41,369 Da), VHL-EloC (29,638 Da), EloC-EloB (22,697 Da), VHL (18,676 Da) and EloB (11,732 Da). An additional 129,257 Da species was also observed that is tentatively assigned as either VHL-EloC-EloB-Cul2 (expected MW 128,558 Da, requires loss of Rbx subunit) or VHL-EloC-Cul2-Rbx1 (expected MW 129,098 Da, requires loss of EloB subunit). The latter complex having a MW more consistent with that observed, but an interesting observation if EloB is the subunit lost from this complex as VCB is a stable trimeric species and more investigation would be required to assign this species. Free Cul2 (87,184 Da), Rbx1 (12,274 Da) or EloC (10,964 Da, as for VCB dissociation) were not observed, **Supporting Information**, **Figure S2** and **Table S5**. Increasing the CID conditions to -125 V (visibility of protein species was lost at -150 V thus not allowing for the direct comparison with VCB), resulted in the observation of the same subunits as described at -75 V as well as the dissociated subunits of Cul2 (89,954 Da), VHL-EloB (30,408 Da), and free EloC (10,962 Da). Additionally, a 113,455 Da species

was observed that could not be assigned to any combination of the subunits, therefore, suggesting CID may have induced subunit fragmentation, however further investigation would be required. The only individual protein subunit not observed following the increased desolvation voltage CID from -75 V to -125 V was free Rbx1 (12, 274 Da).

The binary binding of PROTAC MZ1 and the negative control *cis*-MZ1 to $BRD4^{BD2}$ (POI) with the two E3s (VCB and $CRL2^{VHL}$) was next assessed. Both MZ1 and *cis*-MZ1 bound to $BRD4^{BD2}$, **Figure 4** and **Supporting Information**, **Table S6**. This is consistent with the JQ1 pharmacophore present in both compounds (JQ1 is the pan-BET selective bromodomain inhibitor used in development of MZ1[10, 25, 26]), **Figure 2**. In contrast, binding to VCB or $CRL2^{VHL}$ was observed only with MZ1 and not *cis*-MZ1. This difference is consistent with the inverted stereochemistry of the hydroxyl group of the hydroxyproline moiety of *cis*-MZ1 compared to MZ1 that is known to abolish binding to VHL,[10] **Figure 2.**

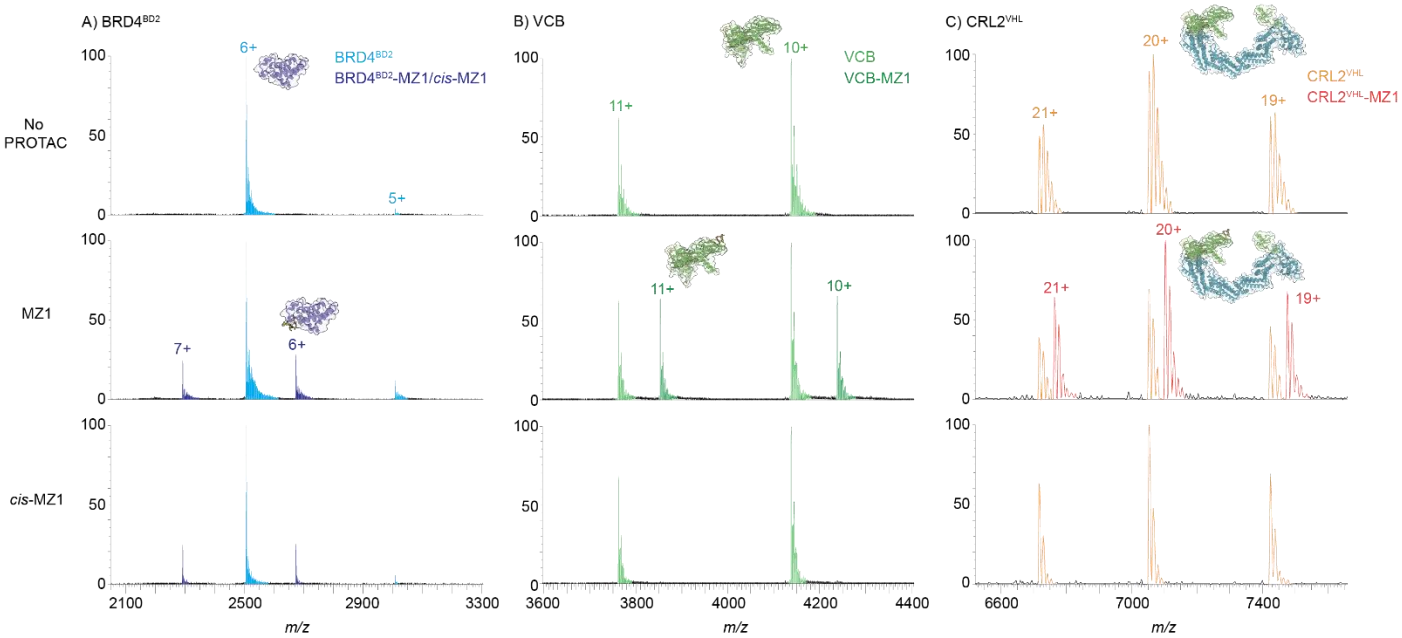

Figure 4. nMS assessment of binary interactions of MZ1 and *cis*-MZ1 (2 µM, 2 equiv) following incubation with 1 µM of A) $BRD4^{BD2}$, B) VCB, or C) $CRL2^{VHL}$ (150 mM NH_4OAc, 1% DMSO). The expected *m/z* shift corresponding to the binding of PROTAC MZ1 was observed in all samples, while the expected *m/z* shift corresponding to the binding of negative control *cis*-MZ1 was observed only with $BRD4^{BD2}$ and not with either E3. Observed *m/z* values are in **Supporting Information**, **Table S6**.

nM analysis of ternary complex formation. For targeted protein degradation, ternary complex formation is critical as the initial target engagement step for subsequent ubiquitination and degradation of the POI. Most methods to screen and characterise potential degrader ligands rely on ternary complex formation as proof of target engagement. Using nMS we observed no interaction of $BRD4^{BD2}$ and VCB without PROTAC, but in the presence of the PROTAC MZ1 the ternary complex $BRD4^{BD2}$-MZ1-VCB was observed (57,409 Da, expected 57,412 Da), consistent with earlier reports.[27, 28] The optimal MZ1 concentration for maximising ternary complex formation over the binary interactions with each protein partner (to diminish the hook effect) was 1.4 equiv, **Figure 5A** and **Supporting Information**, **Table S7** . This concentration was established by titration of MZ1 (1.0-2.0 equiv, in 0.1 increments) against an equimolar mixture of VCB and $BRD4^{BD2}$, **Supporting Information**, **Figure S3** and **S4.** With 1.4 equiv PROTAC minimal free VCB or $BRD4^{BD2}$ were observed, with no binary binding to $BRD4^{BD2}$ but reasonable binary binding to VCB (approx. equal relative intensity to unbound VCB) detected, an indicator of a very strong ternary complex. We re-examined this system with *cis*-MZ1 (1.4 equiv) in place of MZ1 and no ternary complex was observed, while unbound and *cis*-MZ1-bound $BRD4^{BD2}$ and unbound VCB were observed, **Figure 5A**. This confirms the utility of *cis*-MZ1 as a negative control for MZ1 in nMS analysis.

We then assessed if the ternary complex of the full E3 $CRL2^{VHL}$ was observable by nMS. In the absence of PROTAC, there was no interaction between $CRL2^{VHL}$ and $BRD4^{BD2}$, similarly to the corresponding minimal E3 VCB sample, **Figure 5B**. Both free $BRD4^{BD2}$ and $CRL2^{VHL}$ were observed, in addition to minor quantities of VHL-EloC-EloB and Cul2-Rbx1, indicating some dissociation of $CRL2^{VHL}$. On addition of MZ1 (1.4 equiv), the ternary complex comprising $BRD4^{BD2}$-MZ1-$CRL2^{VHL}$ was the major species observed (157,099 Da, expected 157,046 Da), **Figure 5B**. There was some free $CRL2^{VHL}$ observed indicating not all the intact E3 had been recruited into the ternary complex, while lesser amounts of the dissociated subunits VHL-EloC-EloB and Cul2-Rbx1 were also present. Interestingly, there was some ternary complex where the $CRL2^{VHL}$ had dissociated to give VCB (VHL-EloC-EloB) but the ternary complex remained intact (i.e. $BRD4^{BD2}$-MZ1-VCB). Further to this, the complex $BRD4^{BD2}$-VCB was also observed wherein the PROTAC had been dissociated. When replacing MZ1 with the negative control *cis*-MZ1 no ternary complex was observed,

however unbound BRD4^{BD2}, unbound CRL2^{VHL} and unbound dissociated VCB and Cul2-Rbx1 were observed. *cis*-MZ1-bound BRD4^{BD2} was not observed, however it may be too low in intensity relative to background noise in these spectra, **Figure 5B**.

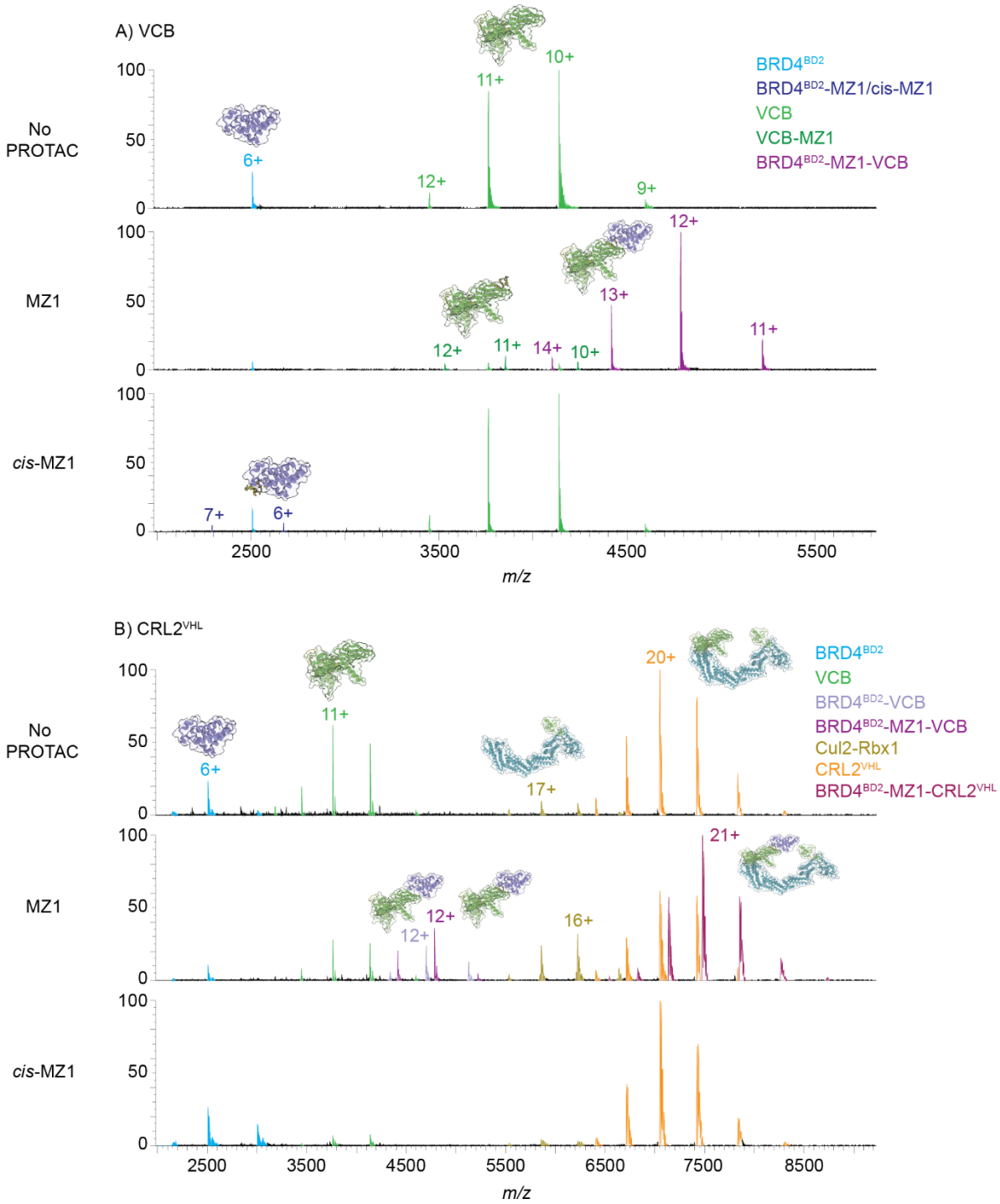

Figure 5. nMS analysis of ternary complex POI-PROTAC-E3 formation between BRD4^{BD2} (1 µM, 1 equiv), MZ1 (1.4 µM, 1.4 equiv) and A) VCB (1 µM, 1 equiv), or B) CRL2^{VHL} (1 µM, 1 equiv) (150 mM NH_4OAc, 1% DMSO). Mass spectra are raw data with charge state and species identity annotated. Top panel is no

PROTAC control (1% DMSO), middle panel is with addition of MZ1, and lower panel is with addition of negative control *cis*-MZ1 (1.4 equiv). Observed *m/z* values are in **Supporting Information**, **Table S7**.

Assessment of the E3-E2 interaction with nMS. The CRL class of E3s transiently recruit an E2 linked to Ub to facilitate Ub transfer to a protein substrate for degradation.[1, 7] nMS analysis of a mixture of $CRL2^{VHL}$ (1 equiv) and an E2 covalently preloaded with Ub, UBE2R1(C93K)-Ub (5 equiv, the Cys to Lys mutation enables covalent loading of a donor Ub[12]) revealed the formation of an E3-E2-Ub complex between $CRL2^{VHL}$ and UBE2R1(C93K)-Ub (177,339 Da, expected 177,254Da), **Figure 6**. The peak intensity for the complex was significant (~15.3% relative intensity), however the major species observed were the free $CRL2^{VHL}$ (with some dissociated VCB) and free E2 UBE2R1(C93K)-Ub (and the minor UBE2R1(C93K) component without Ub conjugated), **Figure 6**. The corresponding raw data mass spectra and observed *m/z* values are shown in **Supporting Information**, **Figure S5** and **Table S8**, respectively. In a physiological setting once E2 transfers the Ub cargo to the substrate, it must dissociate from the E3 to be replenished for next E2-Ub, hence this interaction is transient by nature[7] and therefore exciting to see this interaction was observable by the nMS method, noting it was not possible to capture this interaction by cryo-EM without covalent crosslinking to form the $BRD4^{BD2}$-Ub-E2 conjugated species to artificially increase the occupancy of the E2 on the E3.[12]
The formation of an E3-E2 complex without Ub preloaded onto the E2 was also assessed. Here, UBE2R1(C93K) (2 equiv) was added to $CRL2^{VHL}$ (1 equiv) and a minor amount of E3-E2 complex was observed (167,632 Da, expected 167,638 Da, 5.9% relative intensity), that was similar in intensity to the extent of the complex formed when UBE2R1(C93K)-Ub (2 equiv) was added (3.9% relative intensity) (data not shown). This indicates the transient E3-E2 interactions in this system can be observed regardless of the loading with Ub, despite previous observations that the E3-E2 interaction is stronger in the presence of Ub.[29]

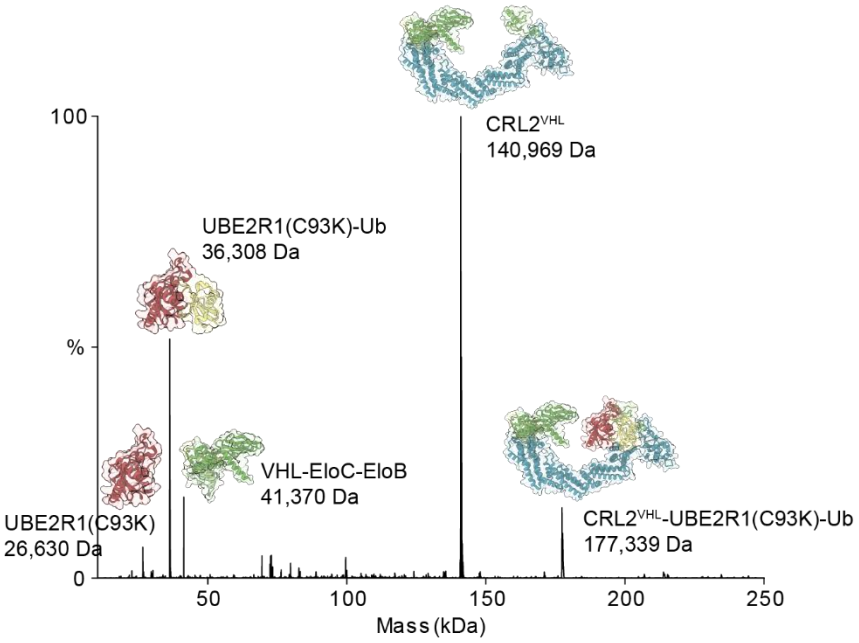

Figure 6. Deconvoluted nMS spectrum of $CRL2^{VHL}$ (1 µM, 1 equiv) in the presence of UBE2R1(C93K)-Ub (5 µM, 5 equiv, 150 mM NH_4OAc). The transient E3-E2-Ub interaction $CRL2^{VHL}$-UBE2R1(C93K)-Ub was observable (177,339 Da). Free $CRL2^{VHL}$ was the major peak observed, with dissociated VHL-EloC-EloB and UBE2R1(C93K)-Ub also observed (with minor UBE2R1(C93K) contaminant). The corresponding raw data mass spectra and observed *m/z* values are shown in **Supporting Information**, **Figure S5** and **Table S8**, respectively.

Assessment of the full $BRD4^{BD2}$-MZ1-$CRL2^{VHL}$-UBE2R1(C93K)-Ub complex with nMS. Next, we investigated the feasibility of capturing the full degradation complex induced by the PROTAC using nMS. For this analysis the sample components were combined in ratios to replicate the conditions used for the cryo-EM study of the related system, **Figure 3**.[12] nMS analysis of the mixture of $BRD4^{BD2}$ (1.5 equiv), the full E3 $CRL2^{VHL}$ (1 equiv) and the Ub-conjugated E2 UBE2R1(C93K)-Ub (5 equiv) in the absence of PROTAC (0.69% DMSO only) showed a low intensity peak corresponding to the $CRL2^{VHL}$-UBE2R1(C93K)-Ub (E3-E2-Ub) complex (observed 177,589 Da, expected 177,465 Da, ~7.7 %, relative intensity), **Figure 7A**. This was consistent with that observed when only the E3 and E2 were combined as described in the previous section, **Figure 6**. Free $BRD4^{BD2}$ (15,036 Da), $CRL2^{VHL}$ (141,020 Da) and UBE2R1(C93K)-Ub (36,308 Da) were readily detected, along with some dissociated VCB (41,374 Da) from the full E3 $CRL2^{VHL}$, **Figure 7A**. Addition of PROTAC MZ1 (1.5 equiv) to this sample resulted in the observation of $BRD4^{BD2}$-MZ1-$CRL2^{VHL}$-

UBE2R1(C93K)-Ub complex (i.e. POI-PROTAC-E3-E2-Ub) (193,479 Da, expected 193,293 Da, 19.6% relative intensity), **Figure 7B**. This corresponds to the full PROTAC-engaged degradation complex that is essential for transferring Ub from the E2 onto the POI. Other species detected in the native mass spectrum included the PROTAC-mediated ternary complex $BRD4^{BD2}$-MZ1-$CRL2^{VHL}$ (157,070 Da) and various dissociated ternary complex species including $BRD4^{BD2}$-MZ1-VHL-EloC-EloB (57,417 Da) and this complex with the PROTAC dissociated (56,415 Da), a phenomenon previously seen in the gas phase nMS measurement of PROTAC ternary complexes.[28, 30-32] Free $BRD4^{BD2}$ (15,037 Da), free E2-Ub UBE2R1(C93K)-Ub (36,308 Da, as well as E2 UBE2R1(C93K) without Ub loaded 26,629 Da) are observed. Interestingly no free E3 $CRL2^{VHL}$ was observed, however, the dissociated subunit complex Cul2-Rbx1 (99,583 Da) was observed. MZ1 was then replaced with *cis*-MZ1, and the results essentially mimicked the DMSO only control, **Figure 7C**. A minor amount of E3-E2-Ub ($CRL2^{VHL}$-UBE2R1(C93K)-Ub) was detected (177,465 Da, ~3.2% relative intensity), however, no ternary complex or ternary complex engaged with E2-Ub was observed. This is consistent with the structural difference of *cis*-MZ1 compared to MZ1 that abolishes VHL-substrate protein binding.[10] The only protein species observed by nMS from this sample were the individual free components $BRD4^{BD2}$ (15,036 Da), $CRL2^{VHL}$ (141,038 Da) and UBE2R1(C93K)-Ub (36,310 Da), as well as some dissociated VCB (41,372 Da) from the full E3 $CRL2^{VHL}$. The corresponding raw data mass spectra and observed *m/z* values are shown in **Supporting Information**, **Figure S6** and **Table S9**, respectively.

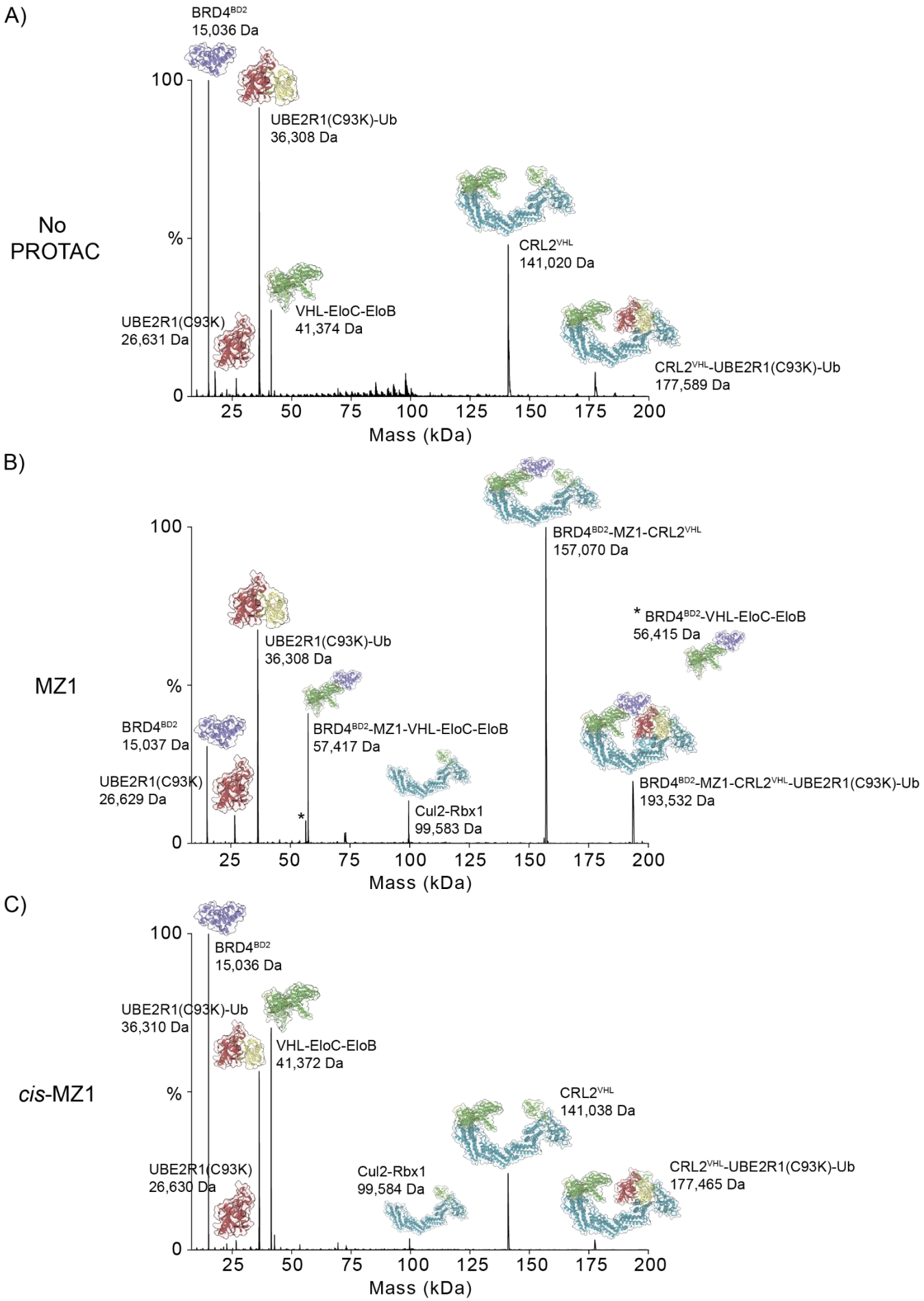
A)
No PROTAC
BRD4BD2
15,036 Da
UBE2R1(C93K)-Ub
36,308 Da
UBE2R1(C93K)
26,631 Da
VHL-EloC-EloB
41,374 Da
CRL2VHL
141,020 Da
CRL2VHL-UBE2R1(C93K)-Ub
177,589 Da
100
%
0
25 50 75 100 125 150 175 200
Mass (kDa)
B)
MZ1
BRD4BD2-MZ1-CRL2VHL
157,070 Da
* BRD4BD2-VHL-EloC-EloB
56,415 Da
UBE2R1(C93K)-Ub
36,308 Da
BRD4BD2
15,037 Da
BRD4BD2-MZ1-VHL-EloC-EloB
57,417 Da
UBE2R1(C93K)
26,629 Da
BRD4BD2-MZ1-CRL2VHL-UBE2R1(C93K)-Ub
193,532 Da
Cul2-Rbx1
99,583 Da
*
100
%
0
25 50 75 100 125 150 175 200
Mass (kDa)
C)
cis-MZ1
BRD4BD2
15,036 Da
UBE2R1(C93K)-Ub
36,310 Da
VHL-EloC-EloB
41,372 Da
CRL2VHL
141,038 Da
UBE2R1(C93K)
26,630 Da
Cul2-Rbx1
99,584 Da
CRL2VHL-UBE2R1(C93K)-Ub
177,465 Da
100
%
0
25 50 75 100 125 150 175 200
Mass (kDa)

Figure 7. Deconvoluted nMS spectra showing PROTAC mediated formation of the BRD4^{BD2}-MZ1-CRL2^{VHL}-UBE2R1(C93K)-Ub complex. A) no PROTAC control (0.69% DMSO), B) with MZ1 (1.5 equiv, 1.5 µM), C) with *cis*-MZ1 (1.5 equiv, 1.5 µM). Protein component ratios of 1.5 equiv BRD4^{BD2} (1.5 µM), 1.5 equiv PROTAC/negative control (1.5 µM), CRL2^{VHL} (1 equiv, 1 µM),UBE2R1(C93K)-Ub (5 equiv, 5 µM) (with final 0.69% DMSO). Raw data mass spectra are shown in **Supporting Information**, **Figure S6**.

Conclusions

Many degraders in development act through the pentameric Cullin RING E3 ligase complex CRL2^{VHL} yet there are few biophysical studies that have characterised this species, with most focusing on the nonfunctional minimal E3 VCB without the Cullin scaffold or RING proteins. Herein we demonstrate the characterisation of CRL2^{VHL} and all expected full E3 complexes integral to the targeted protein degradation mechanism using nMS. This includes the binary, ternary and higher order multiprotein complexes made up of the full E3, POI (BRD4^{BD2}), E2-Ub with and without addition of the PROTAC (MZ1) and covers highly stable complexes through to those expected to be transient and/or weak complexes. We establish direct insight into stoichiometry of interactions and demonstrate the unprecedented advantages of nMS to observe all the expected equilibrium species within a sample in the same measurement, setting nMS apart from other biophysical methods where this is not possible. Whilst high-resolution complex structures provide crucial mechanistic insights into degrader-driven interactions that underpin successful target ubiquitination, the employment of X-ray crystallography or cryo-EM it is not always possible and is not routine. These methods commonly require troubleshooting often against modified protein constructs (including covalent crosslinking to stabilise complexes) to support data collection. As a result, so far there are only a handful of structures of a PROTAC ternary complex wherein a full E3 is used, despite the intensity of research in the field.[12, 33, 34] Given the depth of information achieved from nMS analysis is without resource intensive sample preparation requirements other than standard purified native proteins, we suggest a greater role for nMS in the assessment of multiprotein complex formation to triage degraders, POIs and/or full E3s that are in development for further structural analysis by X-ray crystallography or cryo-EM and/or functional cell-based investigation, with the overall impact of accelerating targeted protein degradation technologies. Future nMS studies may add further

key protein components to the analysis, including NEDD8 modification of the CRL, which is important for activation of the CRL to facilitate Ub transfer.[35]

Supporting Information

Supporting material includes: recombinant $CRL2^{VHL}$ protein production methods; UHMR MS parameters; protein construct sequences, calculated MWs and corrected expected MWs for each protein and protein complex; supporting nMS raw and deconvoluted mass spectra; observed *m/z* values, charge states and MWs for raw and deconvoluted spectra.

Data Availability

The data supporting this study are available in this article and the accompanying online supplementary material. Any addition data is available upon reasonable request from the corresponding authors.

Conflicts of Interest

A.C. is a scientific founder and shareholder of Amphista Therapeutics, a company that is developing targeted protein degradation therapeutic platforms. A.C. is on the Scientific Advisory Board of ProtOS Bio and TRIMTECH Therapeutics. The Ciulli laboratory receives or has received sponsored research support from Almirall, Amgen, Amphista Therapeutics, Boehringer Ingelheim, Eisai, Merck KaaG, Nurix Therapeutics, Ono Pharmaceutical and Tocris Bio-Techne. All other authors declare they have no competing interests.

Funding

The authors greatly acknowledge the support of the Clive and Vera Ramaciotti Foundation (Biomedical Research Award, grant number 2023BRA19) and the Australian Government through an Australian Research Council's Industrial Transformation Training Centre grant (grant number IC180100021). Research in the Ciulli laboratory on Cullin RING ligases and targeted protein degraders, including PROTACs, has received funding from the European Research Council (ERC) under the European Union's Seventh Framework Programme (FP7/2007–2013) as a Starting Grant to A.C. (grant agreement no. ERC-2012-StG-311460

DrugE3CRLs), and from the Innovative Medicines Initiative 2 (IMI2) Joint Undertaking under Grant 875510 (EUbOPEN project). The IMI2 Joint Undertaking receives support from the European Union's Horizon 2020 research and innovation program, EFPIA companies, and associated partners: KTH, OICR, Diamond, and McGill. C. Crowe was supported by a PhD studentship from the UK Medical Research Council (MRC) under the Industrial Cooperative Awards in Science & Technology (iCASE award with Tocris Bio-Techne) doctoral training programme MR/R015791/1 and is now a postdoctoral researcher funded by the Michael J. Fox Foundation.

Acknowledgements

The authors acknowledge opnMe by Boehringer Ingelheim for the complimentary provision of MZ1 and *cis*-MZI. We thank Dr Wendy Loa for mass spectrometry instrumentation support and acknowledge the Ramaciotti Australian Native Mass Spectrometry Platform for Health Discoveries, Griffith University. We thank technical support staff at the University of Dundee for the upkeep of protein production facilities. Molecular graphics of proteins were generated with UCSF ChimeraX, developed by the Resource for Biocomputing, Visualization, and Informatics at the University of California, San Francisco, with support from National Institutes of Health R01-GM129325 and the Office of Cyber Infrastructure and Computational Biology, National Institute of Allergy and Infectious Diseases.[36]

References

[1] Komander, D.; Rape, M. The ubiquitin code. *Annu Rev Biochem* **2012**, *81*, 203-229. DOI: 10.1146/annurev-biochem-060310-170328.
[2] Tsai, J. M.; Nowak, R. P.; Ebert, B. L.; Fischer, E. S. Targeted protein degradation: from mechanisms to clinic. *Nat Rev Mol Cell Biol* **2024**, *25* (9), 740-757. DOI: 10.1038/s41580-024-00729-9.
[3] Li, K.; Crews, C. M. PROTACs: past, present and future. *Chem Soc Rev* **2022**, *51* (12), 5214-5236, 10.1039/D2CS00193D. DOI: 10.1039/D2CS00193D.
[4] Deshaies, R. J. Protein degradation: Prime time for PROTACs. *Nat Chem Biol* **2015**, *11* (9), 634-635. DOI: 10.1038/nchembio.1887.
[5] Hinterndorfer, M.; Spiteri, V. A.; Ciulli, A.; Winter, G. E. Targeted protein degradation for cancer therapy. *Nat Rev Cancer* **2025**, *25* (7), 493-516. DOI: 10.1038/s41568-025-00817-8.
[6] Hughes, S. J.; Ciulli, A. Molecular recognition of ternary complexes: a new dimension in the structure-guided design of chemical degraders. *Essays Biochem* **2017**, *61* (5), 505-516. DOI: 10.1042/ebc20170041.
[7] Deshaies, R. J.; Joazeiro, C. A. RING domain E3 ubiquitin ligases. *Annu Rev Biochem* **2009**, *78*, 399-434. DOI: 10.1146/annurev.biochem.78.101807.093809.
[8] Petroski, M. D.; Deshaies, R. J. Function and regulation of cullin–RING ubiquitin ligases. *Nat Rev Mol Cell Biol* **2005**, *6* (1), 9-20. DOI: 10.1038/nrm1547.

[9] Stebbins, C. E.; Kaelin, W. G., Jr.; Pavletich, N. P. Structure of the VHL-ElonginC-ElonginB complex: implications for VHL tumor suppressor function. *Science* **1999**, *284* (5413), 455-461. DOI: 10.1126/science.284.5413.455.
[10] Zengerle, M.; Chan, K. H.; Ciulli, A. Selective Small Molecule Induced Degradation of the BET Bromodomain Protein BRD4. *ACS Chem Biol* **2015**, *10* (8), 1770-1777. DOI: 10.1021/acschembio.5b00216.
[11] Shrestha, S.; Maitland, M. E. R.; Jing, L.; Duan, S.; Nie, D. Y.; St-Germain, J.; Kanaris, M.; Barsyte-Lovejoy, D.; Arrowsmith, C. H.; Raught, B. Characterization of PROTAC specificity and endogenous protein interactomes using ProtacID. *Nat Commun* **2025**, *16* (1), 8089. DOI: 10.1038/s41467-025-63357-7.
[12] Crowe, C.; Nakasone, M. A.; Chandler, S.; Craigon, C.; Sathe, G.; Tatham, M. H.; Makukhin, N.; Hay, R. T.; Ciulli, A. Mechanism of degrader-targeted protein ubiquitinability. *Sci Adv* **2024**, *10* (41), eado6492. DOI: 10.1126/sciadv.ado6492.
[13] *opnMe® - the open science portal of Boehringer Ingelheim*. https://www.opnme.com/ (accessed 2025).
[14] Marty, M. T.; Baldwin, A. J.; Marklund, E. G.; Hochberg, G. K. A.; Benesch, J. L. P.; Robinson, C. V. Bayesian Deconvolution of Mass and Ion Mobility Spectra: From Binary Interactions to Polydisperse Ensembles. *Anal Chem* **2015**, *87* (8), 4370-4376. DOI: 10.1021/acs.analchem.5b00140.
[15] Tamara, S.; den Boer, M. A.; Heck, A. J. R. High-Resolution Native Mass Spectrometry. *Chem Rev* **2022**, *122* (8), 7269-7326. DOI: 10.1021/acs.chemrev.1c00212.
[16] Bennett, J. L.; Nguyen, G. T. H.; Donald, W. A. Protein–Small Molecule Interactions in Native Mass Spectrometry. *Chem Rev* **2022**, *122* (8), 7327-7385. DOI: 10.1021/acs.chemrev.1c00293.
[17] Hofstadler, S. A.; Sannes-Lowery, K. A. Applications of ESI-MS in drug discovery: interrogation of noncovalent complexes. *Nat Rev Drug Discov* **2006**, *5* (7), 585-595. DOI: 10.1038/nrd2083.
[18] Benesch, J. L. P.; Ruotolo, B. T. Mass spectrometry: come of age for structural and dynamical biology. *Curr Opin Struct Biol* **2011**, *21* (5), 641-649. DOI: https://doi.org/10.1016/j.sbi.2011.08.002.
[19] Faull, S. V.; Lau, A. M. C.; Martens, C.; Ahdash, Z.; Hansen, K.; Yebenes, H.; Schmidt, C.; Beuron, F.; Cronin, N. B.; Morris, E. P.; Politis, A. Structural basis of Cullin 2 RING E3 ligase regulation by the COP9 signalosome. *Nat Commun* **2019**, *10* (1), 3814. DOI: 10.1038/s41467-019-11772-y.
[20] Bulatov, E.; Martin, E. M.; Chatterjee, S.; Knebel, A.; Shimamura, S.; Konijnenberg, A.; Johnson, C.; Zinn, N.; Grandi, P.; Sobott, F.; Ciulli, A. Biophysical studies on interactions and assembly of full-size E3 ubiquitin ligase: suppressor of cytokine signaling 2 (SOCS2)-elongin BC-cullin 5-ring box protein 2 (RBX2). *J Biol Chem* **2015**, *290* (7), 4178-4191. DOI: 10.1074/jbc.M114.616664.
[21] Sternicki, L. M.; Poulsen, S.-A. Native Mass Spectrometry: Insights and Opportunities for Targeted Protein Degradation. *Anal Chem* **2023**, *95* (51), 18655-18666. DOI: 10.1021/acs.analchem.3c03853.
[22] Sternicki, L. M.; Poulsen, S.-A. Toward routine utilisation of native mass spectrometry as an enabler of contemporary drug development. *RSC Med Chem* **2025**, *16* (11), 5114-5124, 10.1039/D5MD00617A. DOI: 10.1039/D5MD00617A.
[23] Sternicki, L. M.; Nonomiya, J.; Liu, M.; Mulvihill, M. M.; Quinn, R. J. Native Mass Spectrometry for the Study of PROTAC GNE-987-Containing Ternary Complexes. *ChemMedChem* **2021**, *16* (14), 2206-2210. DOI: https://doi.org/10.1002/cmdc.202100113.
[24] Gadd, M. S.; Testa, A.; Lucas, X.; Chan, K.-H.; Chen, W.; Lamont, D. J.; Zengerle, M.; Ciulli, A. Structural basis of PROTAC cooperative recognition for selective protein degradation. *Nat Chem Biol* **2017**, *13* (5), 514-521. DOI: 10.1038/nchembio.2329.
[25] Filippakopoulos, P.; Qi, J.; Picaud, S.; Shen, Y.; Smith, W. B.; Fedorov, O.; Morse, E. M.; Keates, T.; Hickman, T. T.; Felletar, I.; Philpott, M.; Munro, S.; McKeown, M. R.; Wang, Y.; Christie, A. L.; West, N.; Cameron, M. J.; Schwartz, B.; Heightman, T. D.; La Thangue, N.; French, C. A.; Wiest, O.; Kung, A. L.; Knapp, S.; Bradner, J. E. Selective inhibition of BET bromodomains. *Nature* **2010**, *468* (7327), 1067-1073. DOI: 10.1038/nature09504.
[26] Wu, Q.; Heidenreich, D.; Zhou, S.; Ackloo, S.; Krämer, A.; Nakka, K.; Lima-Fernandes, E.; Deblois, G.; Duan, S.; Vellanki, R. N.; Li, F.; Vedadi, M.; Dilworth, J.; Lupien, M.; Brennan, P. E.; Arrowsmith, C. H.; Müller, S.; Fedorov, O.; Filippakopoulos, P.; Knapp, S. A chemical toolbox for the study of bromodomains and epigenetic signaling. *Nat Commun* **2019**, *10* (1), 1915. DOI: 10.1038/s41467-019-09672-2.
[27] Beveridge, R.; Kessler, D.; Rumpel, K.; Ettmayer, P.; Meinhart, A.; Clausen, T. Native Mass Spectrometry Can Effectively Predict PROTAC Efficacy. *ACS Cent Sci* **2020**, *6* (7), 1223-1230. DOI: 10.1021/acscentsci.0c00049.

[28] Song, J. H.; Wagner, N. D.; Yan, J.; Li, J.; Huang, R. Y. C.; Balog, A. J.; Newitt, J. A.; Chen, G.; Gross, M. L. Native mass spectrometry and gas-phase fragmentation provide rapid and in-depth topological characterization of a PROTAC ternary complex. *Cell Chem Biol* **2021**, *28* (10), 1528-1538.e1524. DOI: https://doi.org/10.1016/j.chembiol.2021.05.005.
[29] Saha, A.; Deshaies, R. J. Multimodal Activation of the Ubiquitin Ligase SCF by Nedd8 Conjugation. *Molecular Cell* **2008**, *32* (1), 21-31. DOI: 10.1016/j.molcel.2008.08.021.
[30] Maciel, E. V. S.; Eisert, J.; Müller, J.; Habeck, T.; Lermyte, F. Mass Spectrometry Analysis of Chemically and Collisionally Dissociated Molecular Glue- and PROTAC-Mediated Protein Complexes Informs on Disassembly Pathways. *J Am Soc Mass Spectrom* **2025**, *36* (2), 355-367. DOI: 10.1021/jasms.4c00429.
[31] Berwanger, A.; Stein, S. C.; Brandner, S.; Kany, A. M.; Heinz, S.; Loretz, B.; Lehr, C.-M.; Hirsch, A. K. H.; Lermyte, F.; Schulz, T. F.; Empting, M. Toward Anti-Herpesviral PROTACs: Assessing the Challenges for Targeted Protein Degradation on the Example of Kaposi's Sarcoma-Associated Herpesvirus Latency-Associated Nuclear Antigen. *ChemMedChem n/a* (n/a), e202500758. DOI: https://doi.org/10.1002/cmdc.202500758.
[32] Gadallah MI, L. N. K., Nayak D, Zhang P, Dioli O, Zheng G, et al. Unveiling BCL-xL-specific PROTAC Efficiency and Dissociation Mechanisms Using Native Mass Spectrometry. *ChemRxiv* **2025**. DOI: doi:10.26434/chemrxiv-2025-zfjsj
[33] Li, J.; Purser, N.; Liwocha, J.; Scott, D. C.; Byers, H. A.; Steigenberger, B.; Hill, S.; Tripathi-Giesgen, I.; Hinkle, T.; Hansen, F. M.; Prabu, J. R.; Radhakrishnan, S. K.; Kirkpatrick, D. S.; Reichermeier, K. M.; Schulman, B. A.; Kleiger, G. Cullin-RING ligases employ geometrically optimized catalytic partners for substrate targeting. *Mol Cell* **2024**, *84* (7), 1304-1320.e1316. DOI: 10.1016/j.molcel.2024.01.022.
[34] Popow, J.; Farnaby, W.; Gollner, A.; Kofink, C.; Fischer, G.; Wurm, M.; Zollman, D.; Wijaya, A.; Mischerikow, N.; Hasenoehrl, C.; Prokofeva, P.; Arnhof, H.; Arce-Solano, S.; Bell, S.; Boeck, G.; Diers, E.; Frost, A. B.; Goodwin-Tindall, J.; Karolyi-Oezguer, J.; Khan, S.; Klawatsch, T.; Koegl, M.; Kousek, R.; Kratochvil, B.; Kropatsch, K.; Lauber, A. A.; McLennan, R.; Olt, S.; Peter, D.; Petermann, O.; Roessler, V.; Stolt-Bergner, P.; Strack, P.; Strauss, E.; Trainor, N.; Vetma, V.; Whitworth, C.; Zhong, S.; Quant, J.; Weinstabl, H.; Kuster, B.; Ettmayer, P.; Ciulli, A. Targeting cancer with small-molecule pan-KRAS degraders. *Science* **2024**, *385* (6715), 1338-1347. DOI: 10.1126/science.adm8684.
[35] Baek, K.; Krist, D. T.; Prabu, J. R.; Hill, S.; Klügel, M.; Neumaier, L. M.; von Gronau, S.; Kleiger, G.; Schulman, B. A. NEDD8 nucleates a multivalent cullin-RING-UBE2D ubiquitin ligation assembly. *Nature* **2020**, *578* (7795), 461-466. DOI: 10.1038/s41586-020-2000-y.
[36] Meng, E. C.; Goddard, T. D.; Pettersen, E. F.; Couch, G. S.; Pearson, Z. J.; Morris, J. H.; Ferrin, T. E. UCSF ChimeraX: Tools for structure building and analysis. *Protein Science* **2023**, *32* (11), e4792. DOI: https://doi.org/10.1002/pro.4792.